CrossMark

## ORIGINAL ARTICLE

# CPEB4 interacts with Vimentin and involves in progressive features and poor prognosis of patients with astrocytic tumors

Wei Chen[1,2,3] · Zhen Hu[1] · Xi-zhao Li[3] · Jun-liang Li[1,2] · Xin-Ke Xu[2] · Hai-gang Li[4] ·
Yeqing Liu[4] · Bai-hui Liu[5] · Wei-hua Jia[3] · Fang-cheng Li[1,2]

**Abstract** Cytoplasmic polyadenylation element binding protein 4 (CPEB4) is a regulator of gene transcription and has been reported to be associated with biological malignancy in cancers. However, it is unclear whether CPEB4 has any clinical significance in patients with astrocytic tumors, and mechanisms that CPEB4 contribute to progression of astrocytic tumors remain largely unknown. Here, correlation between CPEB4 expression and prognosis of patients with astrocytic tumors were explored by using qPCR, WB and IHC, and X-tile, SPSS software. Cell lines U251 MG and A172 were used to study CPEB4's function and mechanisms. Co-immunoprecipitation, mass spectrometry, immunofluorescent assay, and western blot were performed to observe the interaction between CPEB4 and Vimentin. CPEB4 mRNA and protein levels were markedly elevated in 12/12 astrocytic tumors in comparison to paratumor. High expression of CPEB4 was significantly correlated with clinical progressive futures and work as an independent adverse prognostic factor for overall survival of patients with astrocytic tumors (relative risk 4.5, 95 % CI 2.1–11.2, $p$=0.001). Moreover, knockdown of CPEB4 in astrocytic tumor cells inhibited their proliferation ability, clonogenicity, and invasiveness. Five candidate proteins, GRP78, Mortalin, Keratin, Vimentin, and β-actin, were identified, and the interaction between CPEB4 and Vimentin was finally confirmed. Downregulation of CPEB4 could reduce the protein expression of Vimentin. Our studies first validated that CPEB4 interacts with Vimentin and indicated that high CPEB4 expression in astrocytic tumors correlates closely with a clinically aggressive future, and that CPEB4 might represent a valuable prognostic marker for patients with astrocytic tumors.

**Keywords** Astrocytic tumor · CPEB4 · Vimentin · Prognosis

Wei Chen and Zhen Hu contributed equally to this work.

✉ Wei-hua Jia
  jiaweih@mail.sysu.edu.cn

✉ Fang-cheng Li
  lefangcgz@yeah.net

1   Department of Neurosurgery, Sun Yat-Sen Memorial Hospital, Sun
    Yat-Sen University, No. 107 West Road of Riverside,
    Guangzhou 510120, China

2   Department of Neurosurgery, Guangzhou Women and Children's
    Medical Center, No. 9 Jinsui Road, Guangzhou 510623, China

3   State Key Laboratory of Oncology in South China, Sun Yat-Sen
    University Cancer Center, 651 Dongfeng East Road,
    Guangzhou, China

4   Department of Pathology, Sun Yat-Sen Memorial Hospital, Sun
    Yat-Sen University, No. 107 West Road of Riverside,
    Guangzhou 510120, China

5   Department of General Surgery, The Second Affiliated Hospital of
    GuangDong Pharmaceutical University, No. 167 Xingang Xi Road,
    Guangzhou 510275, China

## Introduction

Astrocytic tumors, also known as astrocytomas, are the most common tumors of the central nervous system and are defined by their composition of neoplastic astrocytes and include subependymal giant cells, pilocytic astrocytomas, pilomyxoid astrocytomas, diffuse astrocytomas, pleomorphic xanthoastrocytomas, anaplastic astrocytomas, glioblastomas, giant cell glioblastomas, and gliosarcomas. Malignant astrocytic tumors account for approximately 70 % of adult malignant primary brain tumors and are one of the most destructive neoplasms [1]. Despite the progress that has been made in surgery and chemoradiotherapy in recent years, the overall survival time of this disease remains poor [2], and low-grade gliomas eventually progress into high-grade gliomas [3]. The

🖉 Springer

detection of human gene mutations associated with brain tumorigenesis may enable the stratification of patients based on their molecular classification, complementing traditional histology-based categorizations and possibly producing new therapeutic strategies [4–7]. However, thus far, there is still a lack of specific and/or sensitive biomarkers for the precise prediction of clinical outcomes in astrocytic tumors. Therefore, it is necessary to develop effective markers with increased specificity and/or sensitivity for the clinical evaluation of prognosis in astrocytic tumors [8–11].

Cytoplasmic polyadenylation element binding protein 4 (CPEB4) is an 80.2-kDa protein of the CPEB family, which mainly regulates translation by controlling the polyadenylation of target genes [12, 13]. In recent years, data have shown that CPEB4 not only is expressed in a variety of somatic tissues but also has essential functions in regulating the balance between senescence and proliferation and its pathological manifestation and tumor development [14–17]. Furthermore, CPEB4 has been found to mediate the pathological activation of tissue plasminogen activator (tPA) mRNA in pancreatic ductal adenocarcinoma (PDA). To date, however, there is limited knowledge on CPEB4 abnormalities and its clinical implications in patients with astrocytic tumors. In our study, we performed a correlative analysis on CPEB4 expression and clinical data to evaluate whether the expression of CPEB4 could predict the prognosis of patients with astrocytic tumors. The function and mechanism of CPEB4 also been explored in this study.

## Materials and methods

### Patient and tissue microarray

We collected a total of 200 paraffin-embedded glioma tissues from May 2004 to September 2012, all these samples with complete clinical pathological data (detailed in Table 1). Twelve normal brain tissues were from the patients with craniocerebral trauma between July 2013 and June 2014, and these tissues were used as normal controls and confirmed to be free of any detectable pathological conditions. Twelve fresh glioma tissues were from patients who underwent surgery between July 2013 and June 2014 and all diagnosed with astrocytic tumors. All the fresh samples were kept in liquid nitrogen before the experiments were performed. According to the 2007 WHO classification of tumors of the central nervous system, of the 200 glioma tissues, 17 were grade I, 100 were grade II, 36 were grade III, and 47were grade IV. Patients' clinicopathological data including patient age, sex, tumor location, tumor size and 2007 WHO grade, extent of surgical resection, and KPS score before operation; symptom of intracranial hypertension; symptom of epilepsy; and the survival time after surgery were collected. None of the cancer patients had received preoperative radiation or chemotherapy.

All samples were histopathologically diagnosed and anonymized at the Department of Pathology, The Second Affiliated Hospital, Sun Yat-Sen University. The medical ethics committee of The Second Affiliated Hospital, Sun Yat-Sen University approved this study. All of the patients involved in this study have given consents and approved the present study.

Tissue microarray (TMA) was constructed as the method described previously [18]. Briefly, the TMA block contained 600 (200×3) spots from 200 glioma tissues, and the locations were arranged according to the hospital numbers. Corresponding hematoxylin and eosin (H&E)-stained slides and formalin-fixed, paraffin-embedded tissue blocks were used for TMA sampling. A pathologist reviewed the H&E slides to mark out representative tumor areas. By using a tissue arraying instrument (Alphelys, MiniCore), triplicate cylindrical tissue specimens of 1.0 mm diameter were punched from representative tumor areas of individual donor tissue block then re-embedded into a recipient paraffin block at a defined position. This study included only 573 (191×3) cases, nine cases included samples with too few tumor cells (<300 cells per case) and unrepresentative areas, and lost samples were excluded. A total of 480 (160×3) of the astrocytic tumor spots underwent statistical analysis, and all other histologic glioma subtypes were excluded.

### qRT-PCR analysis

qRT-PCR analysis was performed to test mRNA expression in this study. Total RNA was extracted with TRIzol reagent (Invitrogen, CA, USA) from 12 pairs of fresh astrocytic tumor tissues and normal brain tissues, and synthesized into cDNA with the PrimeScript RT reagent Kit (TaKaRa, Japan). The CPEB4 primers were 5′-TGCTATCCATTCTCGTGCTG-3′ and 5′-AGCGTGAAGAGGTTGAGGAA-3′. The Vimentin (VIM) primers were 5′-TGTCCAAATCGATGTGGATGT TTC-3′ and 5′-TTGTACCATTCTTCTGCCTCCTG-3′; the β-actin primers were 5′-TAGCACAGCCTGGATAGCA ACGTAC-3′ and 5′-CACCTT CTACAATGAGCT GCGTGTG-3′. qRT-PCR was performed with SYBR Green PCR master mix (Applied Biosystems, USA) in a total volume of 20 μl on the Light-Cycler 480 instrument (Roche Diagnostics, Penzberg, Germany), and it was initiated at 95 °C for 10 min, 45 cycles of 95 °C for 20 s, 60 °C for 20 s, and 72 °C for 30 s, and a final extension step of 72 °C for 3 min.

### Western blot analysis

Samples from the 12 pairs of fresh astrocytotic tumor tissues and normal brain tissues weighed ~20 mg and were then washed twice with PBS and homogenized by RIPA buffer (50 mM of Tris, pH 7.4, 250 mmol/l of NaCl, 5 mmol/l of

**Table 1** Correlation between CPEB4 expression and clinicopathological characteristics of patients with astrocytic tumors

| Characteristics | CPEB4 protein | | | p value[a] |
|---|---|---|---|---|
| | Total (n=160) | Low (%) | High (%) | |
| Age (years)[b] | | | | 0.076 |
| ≤38 | 77 | 54 (33.8) | 23 (14.4) | |
| >38 | 83 | 35 (21.9) | 48 (30.0) | |
| Gender | | | | 0.628 |
| Female | 65 | 38 (23.8) | 27 (16.9) | |
| Male | 95 | 51 (31.9) | 44 (527.) | |
| KPS[c] | | | | 0.016 |
| ≤70 | 91 | 43 (26.9) | 48 (30.0) | |
| >70 | 69 | 46 (28.8) | 23 (14.4) | |
| 2007 WHO grade | | | | <0.001 |
| I | 11 | 10 (6.2) | 1 (0.6) | |
| Subependymal giant cell astrocytoma | 6 | | | |
| Pilocytic astrocytoma | 5 | | | |
| II | 76 | 73 (46.2) | 3 (1.9) | |
| Pilomyxoid astrocytoma | 23 | | | |
| Diffuse astrocytoma | 33 | | | |
| Pleomorphic xanthoastrocytoma | 21 | | | |
| III | 27 | 3 (1.9) | 24 (15.0) | |
| Anaplastic astrocytoma | 27 | | | |
| IV | 46 | 3 (1.2) | 43 (26.9) | |
| Glioblastoma | 35 | | | |
| Giant cell glioblastoma | 7 | | | |
| Gliosarcoma | 4 | | | |
| Tumor size (cm)[d] | | | | 0.014 |
| ≤5 | 80 | 50 (31.2) | 30 (18.8) | |
| >5 | 80 | 39 (24.4) | 41 (25.6) | |
| Tumor location | | | | 0.224 |
| Supratentorial | 22 | 17 (10.6) | 5 (3.1) | |
| Infratentorial | 138 | 72 (45.0) | 66 (41.2) | |
| Intracranial hypertension symptom | | | | 0.004 |
| No | 77 | 52 (32.5) | 25 (15.6) | |
| Yes | 83 | 37 (23.1) | 46 (28.8) | |
| Epilepsy symptom | | | | <0.001 |
| No | 110 | 50 (31.2) | 60 (37.5) | |
| Yes | 50 | 39 (24.4) | 11 (6.9) | |

[a] Chi-square test

[b] Median age

[c] Median KPS score

[d] Median size

EDTA, 1 % NP40, 0.1 % sodium dodecyl sulfate, 0.5 % sodium deoxycholate, and 1 mmol/l of phenylmethylsulfonyl fluoride) on ice for 45 min. The lysates were processed in a centrifuge at 13,000×g for 10 min at 4 °C, and the protein concentration was determined using the BCA protein assay kit (Pierce Chemical Company, Rockford, IL, USA). Twenty micrograms of total protein was subjected to sodium dodecyl sulfate-polyacrylamide gel electrophoresis and transferred to a polyvinylidene fluoride membrane. Cultured tumor cells were washed twice with PBS and lysed in radioimmune precipitation assay buffer for 30 min on ice. Cell lysates were clarified by processing them in a centrifuge at 13,000×g for 10 min at 4 °C, and the protein concentration was determined using the BCA protein assay kit (Pierce Chemical Company, Rockford,

IL, USA). Thirty micrograms of total protein was subjected to sodium dodecyl sulfate-polyacrylamide gel electrophoresis and transferred to a polyvinylidene fluoride membrane. Rabbit antibody against CPEB4 antibodies (1:5000 dilution, Cat#ab155204; Abcam, UK) and mouse monoclonal Vimentin antibody (1:5000 dilution, Cat#ab8069; Abcam, UK) were used to detect the CPEB4 and Vimentin protein, respectively. β-Actin antibody (1:5000 dilution, Cat#ab6276; Abcam, UK) was used as internal protein control. Specific proteins were detected by enhanced chemiluminescence Kit (Pierce Chemical Company) according to the manufacturer's instructions. Density of the bands imaged by x-ray films was obtained by ImageJ.

## Immunohistochemistry staining and evaluation

Four- to five-micrometer-thick TMA slides were used for CPEB4 IHC staining. Slides were dried for 2 h at 60 °C, deparaffinized in xylene followed by rehydration through graded alcohol (100, 95, and 85 % for 5 min each), immersed in 3 % hydrogen peroxide for 15 min for endogenous peroxidase blocking, and placed into the ethylenediamine tetraacetic acid (EDTA) buffer (pH=8.0) by treatment with pressure cooking for 4 min for antigen retrieval. Then, 10 % normal goat serum was pre-incubated at room temperature for 30 min for blocking binding of non-specific reaction. A rabbit antibody against CPEB4 (1:200, Cat#ab155204; Abcam, UK) was used as primary antibody at 4 °C overnight. Normal murine IgG was used as negative controls and human placenta sections (obtained from the Department of Pathology, The Second Affiliated Hospital, Sun Yat-Sen University) were used as positive controls. A goat anti-rabbit immunoglobulin G (ZSGB-BIO, Beijing, China) was incubated with the slides for 1 h and 30 min at room temperature, and staining was performed with DAB (3,3-diaminobenzidine) for 10 s. Finally, the slides were counterstained with diaminobenzidine (ZSGB-BIO, Beijing, China) and Meyer's hematoxylin (BASO diagnostics, Inc., Zhuhai, China), dehydrated, and mounted.

All TMA slides were examined by two independent, blinded investigators randomly using an Olympus BX51 digital photomicroscope. Intensity score from 0 to 3 ($I_0$, negative staining; $I_1$, weak, light yellow staining; $I_2$, moderate, yellow-brown staining; $I_3$, strong, brown staining) and proportion of tumor cells were recorded as 5 % increments from a range of 0–100 ($P_0$, $P_{1-3}$). Finally, the sum of scores from each intensity and proportion of area stained was added as an H score (H score=$I_1 \times P_1 + I_2 \times P_2 + I_3 \times P_3$, range 0–300).

## Cell culture

The two typical astrocytic tumor cell lines (U251 MG and A172) were purchased from the Shanghai Institute of Cytobiology. They were maintained in DMEM (Gibco BRL, Carlsbad, CA, USA) and supplemented with 10 % fetal bovine serum (FBS), 100 U/ml penicillin, 100 μg/ml streptomycin, and 0.25 mmol/l L-glutamine in a humidified incubator at 37 °C and 5 % $CO_2$. These two cell lines were regularly authenticated by morphologic observation and tested for absence of mycoplasma contamination (MycoAlert, Lonza). Cells in the exponential growth phase were used for all experiments.

## Downregulation of CPEB4 using si-h-RNA in astrocytic tumor cells

The U251-MG and A172-MG cells were seeded in six-well plates and cultured for 24 h before use. CPEB4 specific si-h-RNA were purchased from Ribobio (Guangzhou, China) as listed: NControl#siN05815122147, si-h-CPEB4-101#siG000080315A, si-h-CPEB4-102#siG000080315B, and si-h-CPEB4-103#siG000080315C. The greatest reduction of CPEB4 concentrations si-h-CPEB4_102 and si-h-CPEB4_103 was selected for further experiments. Lipofectamine 3000 (Invitrogen, Carlsbad, CA, USA) was used to transfect si-h-RNA into cells following the manufacturer's instructions. Forty-eight hours after transfection, the cells were collected and used for the further experiments.

## MTT assay

U251 MG-siBlank, U251 MG-siNControl, U251 MG-si-h-CPEB4-102, U251 MG-si-h-CPEB4-103 and A172-siBlank, A172-siNControl, A172-si-h-CPEB4-102, A172-si-h-CPEB4-103 cells were processed for cell proliferation analysis in the MTT assay. Cells were reseeded in 96-well plates ($2 \times 10^3$ cells/well) after transfection and incubated overnight. To measure cell growth, 20 μl 5 mg/ml 3-(4,5-dimethyl-thiazol-2-yl)-2,5-diphenyltetrazolium bromide (MTT; Sigma-Aldrich, USA) was added into the media and cultured at 37 °C for 4 h. Then 150 μl dimethyl sulfoxide (MPBIO, cat no. 196055) was added to resolve the generated formazan right after removing the cell medium, and the OD570 value of the solvent was measured with a microplate reader (MULTISKAN MK3; Thermo, USA). To generate a cell growth curve, the measurement process was performed every 24 h for 6 days and each experiment was repeated at least three times.

## Colony formation assay

For colony-forming assays, U251 MG-siBlank, U251 MG-siNControl, U251 MG-si-h-CPEB4-102, U251 MG-si-h-CPEB4-103 and A172-siBlank, A172-siNControl, A172-si-h-CPEB4-102, A172-si-h-CPEB4-103 cells were seeded in six-well plates at 1000 cells per well, with medium replacement every 3 days. After incubating at 37 °C for 2 weeks, the

surviving colonies (>50 cells per colony) were stained with 0.1 % crystal violet solution (Sigma-Aldrich, MO, USA) and scored while being viewed under a microscope. All experiments were done in triplicate.

## The Transwell invasion assay

The cell invasion assay was carried out using wells (Corning Costar Corp., Cambridge, MA) which were coated with pre-diluted Matrigel (BD Biosciences, Bedford, MA). Approximately $2 \times 10^5$ astrocytotic tumor cells were seeded into upper wells which was filled with 200 μl DMEM supplemented with 10 % FBS, and the lower chamber of the Transwell was filled with 500 μl of serum-free DMEM. Incubated for 14 h at 37 °C, cells that did not invade through the Matrigel to the bottom of the insert were removed gently with a cotton swab. Cells that invaded to the lower side of the membrane were fixed with 95 % methanol, stained with 0.1 % crystal violet (Sigma-Aldrich, MO, USA), photographed under a microscope, and quantified by counting cells manually in three random areas. All experiments were done in triplicate.

## Immunoprecipitation and protein separation

Briefly, 4 μg of anti-CPEB4 antibody (Cat#ab155204; Abcam, UK) was incubated with the agarose conjugate with gentle rotation at 4 °C overnight. Then 1 mg protein lysate from the astrocytotic tumor cells (shCPEB4 and NC group) was added to the agarose conjugate/antibody complex rotation overnight at 4 °C and centrifuged at 3000×g for 2 min to collect immunoprecipitated complexes, and the supernatant was discarded. The pellet was washed with 1 ml phosphate buffered saline and centrifuged at 3000×g for 2 min at 4 °C three times, then 20–100 μl Laemmli sample buffer was added to the tube and resuspended each pellet. Samples were heated at 95 °C for 5 min. Twenty microliters of the sample was loaded on a 10 % gel and run under reducing conditions for SDS-PAGE.

## Band picking and enzymatic digestion

The gel was stained with silver to visualize the bands; this process was performed according to the manufacturer's protocol (Silver Quest™ Silver Staining Kit Manual, IM-6070; Life Company, USA). The differentially abundant protein bands were selected and excised carefully from the silver-stained preparative gel into new tubes. The bands were cut into pieces gently and washed with Milli-Q water twice; 50 % acetonitrile (ACN) and 50 mM ammonium bicarbonate ($NH_4HCO_3$) were added to destain the bands and then dried in 37 °C conditions. Moreover, 10 mM DL-dithiothreitol and 50 mM $NH_4HCO_3$ were added to the proteins within the gel pieces and incubated for 30 min at 56 °C, then the protein samples were alkylated by

incubation under dark conditions with 55 mM iodoacetamide in 50 mM $NH_4HCO_3$ for 30 min. Fifty percent acetonitrile was added to dehydrate the samples then rehydrated in 100 mM $NH_4HCO_3$; this process was performed twice. The gel pieces were dehydrated in acetonitrile and then incubated in trypsin (Sigma-Aldrich, CA, USA) for 30 min at 4 °C then put in 37 °C conditions overnight. Then into the samples were added 10 % ACN, 50 mM $NH_4HCO_3$, and Milli-Q water. In addition, 2.5 % trifluoroacetic acid/90 % acetonitrile were used for extracting peptide mixtures at room temperature for 30 min, and the samples were dried at 37 °C conditions.

## Protein band identification by mass spectrometry

Milli-Q water and 0.1 % trifluoroacetic acid/30 % acetonitrile were added to the samples to dissolve the peptide material. Then, 0.7 μl mixture with 0.4 μl 5 mg/ml alpha-cyano-4-hydroxycinnamic acid matrix was loaded to a target plate and dried at room temperature, and then analysis was performed using MALDI-TOF/TOF proteomics mass spectrometer system (Bruker Daltonics, Germany). The mass spectrometry data were matched to the peptide mass database (*Toxoplasma gondii* protein database, www.toxodb.org; NCBI databases, www.ncbi.nlm.nih.gov/BLAST) and analyzed by using FlexAnalysis 3.3 software (Bruker Daltonics, Germany). The Mascot software (http://www.matrixscience.com) was used to carry out protein identification with MALDI-TOF MS. A Mascot confidence interval of 95 % and protein scores greater than 60 are considered significant ($p<0.05$).

## Immunofluorescence staining and fluorescence microscopy

A172 cells were seeded to coverslips and incubated for 24 h at 37 °C. Cells were washed three times with PBS and then fixed in 4 % paraformaldehyde (Sigma-Aldrich, MO, USA) for 20 min at room temperature. Then 0.3 % Triton X-100 (Sigma-Aldrich, MO, USA) with PBS was used to permeabilize the fixed cells. Ten percent normal goat serum (Sigma-Aldrich, MO, USA) was used for pre-incubation at room temperature for 30 min for blocking binding of non-specific reaction. Then the cells were incubated with mixed primary antibodies (CPEB4, Vimentin, 1:150 dilutions) at 4 °C overnight. The cells were washed with PBS three times and then incubated with DyLight 594 AffiniPure Goat Anti-Rabbit IgG(H+L) and DyLight 488 AffiniPure Goat Anti-Mouse IgG(H+L) (Sigma-Aldrich, MO, USA) and at 1:1000 dilution for 1 h at 37 °C at a dark condition. Also, 1 μg/ml DAPI (Sigma-Aldrich, MO, USA) was used for staining the nuclei and incubated for 5 min at room temperature. The staining is evaluated using fluorescence microscopy (Olympus IX71).
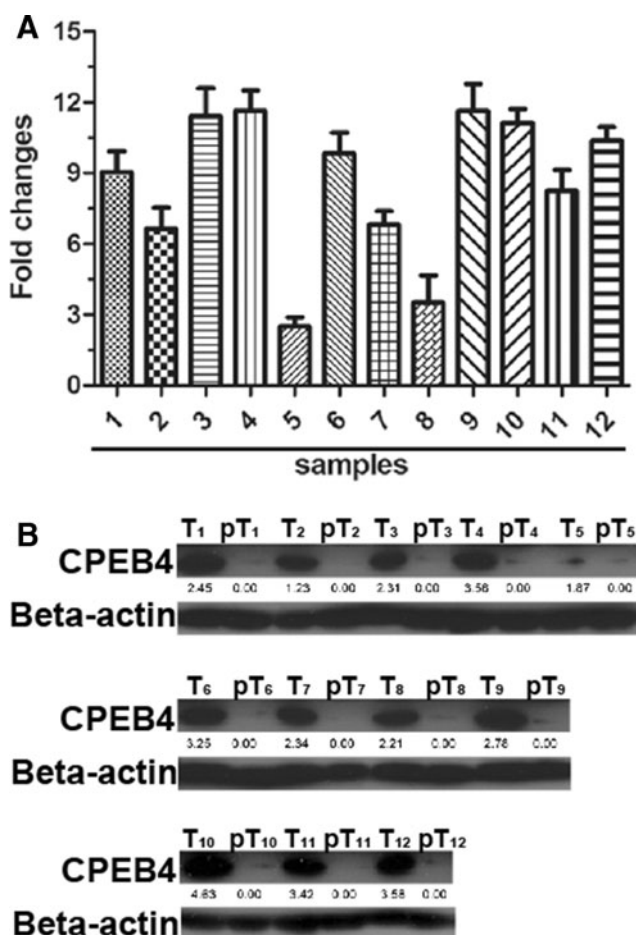
**Fig. 1** **a** Representative qRT-PCR. Upregulated expression of CPEB4 mRNA was examined by qRT-PCR in 12/12 astrocytomas cases, when compared with paired normal brain tissues. Expression levels were normalized for β-actin. *Error bars*, SEM calculated from three parallel experiments. The average changed fold was 8.62 ($p < 0.001$). **b** Representative Western blots. Upregulated expression of CPEB4 protein was detected by Western blotting in 12/12 astrocytomas cases, when compared with paired normal brain tissues. Expression levels were normalized with GAPDH. The average changed fold was 2.80 ($p < 0.001$)

## X-tile analysis

The optimal cut-off point for CPEB4 expression was obtained using X-tile software version 3.6.1 (Yale University School of Medicine, New Haven, CT, USA), as previously described. CPEB4 expression assessment was performed by creating X-tile plots in which cut points were optimized based on clinical outcome. The cut-off score derived from 160 samples was performed for assessing statistical significance.
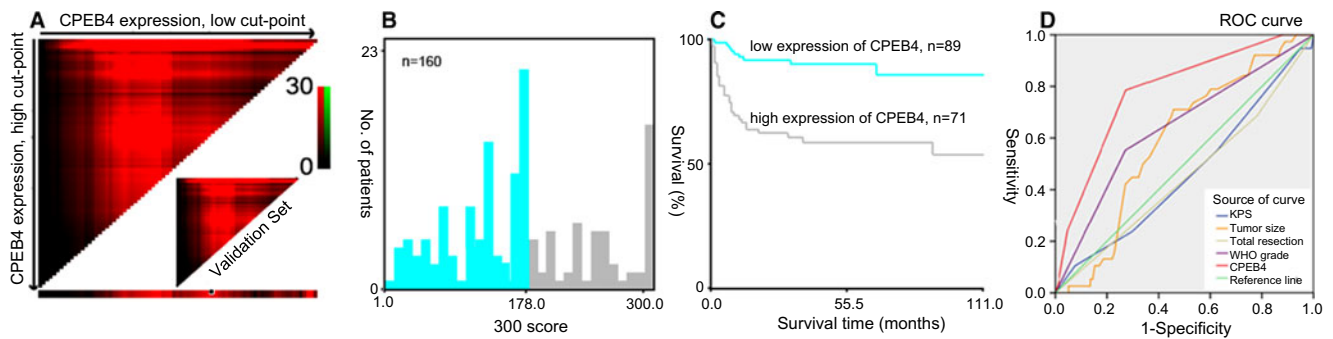
## Statistical analysis

mRNA and protein expression levels of CPEB4 were analyzed using the *t* test. Associations between clinicopathologic factors and survival were evaluated using the Cox proportional hazard model. The hazard ratio (HR) and 95 % confidence

interval (CI) were assessed for each factor. Receiver operating characteristic (ROC) curve analysis was performed to evaluate the predictive value of the parameters. The relationships between the expression levels of CPEB4 and tPA were assessed using Pearson's correlation coefficients and linear regression analyses. All statistical analysis was performed using SPSS (SPSS Standard version 16.0; SPSS, Chicago, IL, USA). All
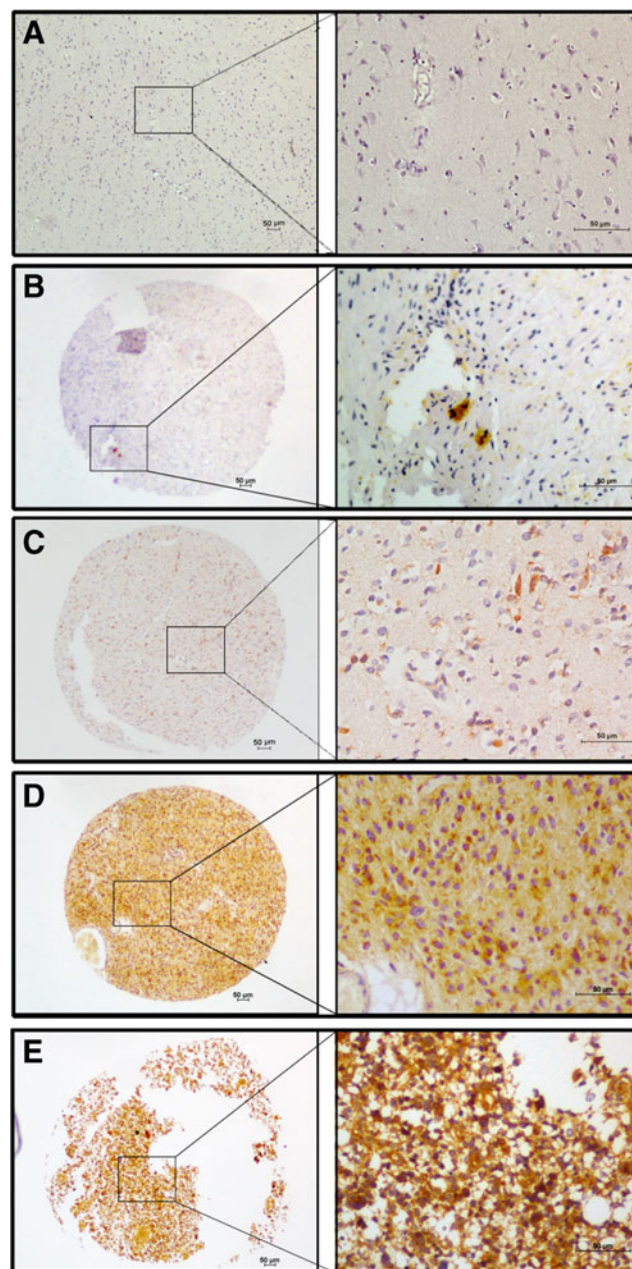


**Fig. 2** Representative photographs of the expression of CPEB4 in astrocytic tumor tissues and paratumor tissues by IHC (×40 and ×200). **a** Normal brain tissue, **b** subependymal giant cell astrocytoma (WHO I), **c** diffuse astrocytoma (WHO II), **d** anaplastic astrocytoma (WHO III), and **e** glioblastoma (WHO IV). CPEB4 expression was significantly increased with the increasing pathologic grades ($p < 0.001$)

**Fig. 3** Statistical analysis of the prognostic marker CPEB4 on 160 patients with astrocytic tumors. **a** X-tile plots of training sets, with matched validation sets in the smaller inset. The plot showed the $\chi^2$ log-rank values generated when dividing the cohort into two populations. **b** The cut point (H score=178) highlighted by the *black/ white circle* in the horizontal axis was demonstrated on a histogram of the entire cohort. **c** The Kaplan-Meier curves show that patients with high CPEB4 expression have poor overall survival (analysis of 160 astrocytomas tissues; $p<0.001$). **d** ROC curve analysis for different clinicopathological features and CPEB4 expression was performed to evaluate the survival status. KPS (AUC=0.435; $p=0.432$), WHO grade (AUC=0.597; $p=0.004$), total resection (AUC=0.463; $p=0.269$), CPEB4 (AUC=0.746; $p<0.001$)

tests were two-sided, and a $p$ value of less than 0.05 was considered statistically significant.

## Results

### Expression of CPEB4 in astrocytic tumor tissues

CPEB4 mRNA was overexpressed in all of the 12 paired astrocytic tumor samples, and the average fold change was 8.62 ($p<0.001$) (Fig. 1a). CPEB4 protein was also upregulated in 12/12 paired astrocytic tumor samples, and the average fold change was 2.80 ($p<0.001$) (Fig. 1b).

In the IHC analysis, CPEB4 protein in glioma tissues mainly accumulated in the cytoplasm and, to a lesser extent, in the nucleus (Fig. 2b–e). Compared to grade I–II gliomas (Fig. 2b, c), grade III–IV gliomas (Fig. 2d, e) had more cells with positive CPEB4 immunostaining and stronger staining intensities; however, the normal brain tissue showed negative CPEB4 immunostaining (Fig. 2a). H scores above the cutoff point value of 178 were defined as being of high expression according to the X-tile program (Fig. 3a–c). Increased CPEB4 expression was found in 71/160 (44.4 %) of the astrocytic tumors. Correlations between CPEB4 expression and patient characteristics are listed in Table 1.

### Associations between CPEB4 expression and clinicopathological variables

In a univariate survival analysis, it was found that significantly increased CPEB4 correlated with increasing pathologic grades ($p<0.001$). CPEB4 expression levels were also significantly associated with KPS status ($p=0.016$), tumor size ($p=0.014$), intracranial hypertension symptoms ($p=0.004$), and epilepsy ($p<0.001$). However, no significant differences were found between CPEB4 expression and other clinicopathological

variables, including patients' sex ($p=0.628$), age ($p=0.076$), and tumor location ($p=0.224$). The associations between CPEB4 expression levels and clinicopathological variables are summarized in Table 2.

### Prognostic value of CPEB4

The results of a Kaplan-Meier analysis indicated that here was a significant impact of well-known clinical pathological prognostic parameters on patient survival, including KPS scores ($p<0.001$), WHO grades ($p<0.001$), tumor size ($p=0.014$), intracranial hypertension symptoms ($p=0.004$), and epilepsy symptoms ($p<0.001$). A significant correlation was found between high CPEB4 expression and poor survival of astrocytic tumor patients ($p<0.001$, Fig. 3c, Table 2).

Multivariate analysis showed that high CPEB4 expression emerged as a significant independent poor prognostic factor in astrocytic tumor patients (relative risk 4.5, 95 % CI 2.1–11.2, $p=0.001$, Table 2). As for other factors, only KPS status (relative risk 0.1, 95 % CI 0.0–0.3, $p=0.005$, Table 2) and WHO grade ($p=0.019$, Table 2) proved to have any independent prognostic value for overall survival prediction.

A ROC curve was constructed to evaluate the prognostic value between CPEB4 expression levels and patient survival status. In our results, CPEB4 was found to be a promising predictor of astrocytic tumor patient survival status [area under curve (AUC)=0.746, $p<0.001$, Fig. 3d].

### Characterization of the effects of CPEB4 knockdown in typical astrocytic tumor cells

In three different CPEB4-targeting si-h-RNAs (si-h-CPEB4_101 through si-h-CPEB4_103) and the parental glioma cells transfected with NControl, the expression of CPEB4 mRNA was efficiently downregulated ($p<0.05$, Fig. 4a). We selected the greatest reduction of CPEB4, si-h-CPEB4_102

**Table 2** Univariate and multivariate analysis of different prognostic factors in 160 patients with astrocytic tumors

| Characteristics | Univariate analysis | | | Multivariate analysis | | |
|---|---|---|---|---|---|---|
| | | Total | *p* value | Hazard ratio | 95 % CI | *p* value |
| Age (years)[a] | | | 0.145 | | | |
| ≤38 | 77 | 1 | | | | |
| >38 | 83 | 1.7 (0.9–3.2) | | | | |
| Gender | | | 0.171 | | | |
| Female | 65 | 1 | | | | |
| Male | 95 | 1.5 (0.8–3.0) | | | | |
| KPS | | | <0.001 | 0.1 | 0.0–0.3 | 0.005 |
| ≤70 | 91 | 1 | | | | |
| >70 | 69 | 0.2 (0.0–0.3) | | | | |
| WHO grade | 160 | | <0.001 | | | |
| I | 11 | 1 | | | | 0.019 |
| II | 76 | 1.8 (0.2–13.4) | | 1.9 | 0.3–15.1 | 0.489 |
| III | 27 | 6.3 (0.8–59.4) | | 6.8 | 0.9–52.8 | 0.058 |
| IV | 46 | 11. 3 (1.4–77.3) | | 8.9 | 1.2–65.8 | 0.029 |
| Tumor size (cm)[b] | | 0.008 | | 1.8 | 1.0–3.5 | 0.063 |
| ≤5 | 80 | 1 | | | | |
| >5 | 80 | 2.4 (1.3–4.4) | | | | |
| Tumor location | | | 0.186 | | | |
| Supratentorial | 22 | 1 | | | | |
| Infratentorial | 138 | 2.4 (0.9–8.2) | | | | |
| Total resection | | | 0.086 | | | |
| No | 44 | 1 | | | | |
| Yes | 116 | 0.5 (0.2–1.2) | | | | |
| Intracranial hypertension symptom | | | 0.031 | 1.1 | 0.6–2.2 | 0.771 |
| No | 77 | 1 | | | | |
| Yes | 83 | 2.1 (1.3–3.8) | | | | |
| Epilepsy symptom | | | 0.003 | 0.6 | 0.3–1.6 | 0.363 |
| No | 110 | 1 | | | | |
| Yes | 50 | 0.3 (0.1–0.7) | | | | |
| CPEB4 | | | <0.001 | 4.5 | 2.1–11.2 | 0.001 |
| Low | 97 | 1 | | | | |
| High | 63 | 3.6 (2.3–6.4) | | | | |

*HR* hazards ratio, *CI* confidence interval

[a] Median age

[b] Median size

and si-h-CPEB4_103 concentrations for further experiments. Western blot analyses showed that CPEB4 protein concentrations were downregulated in control cells and in cells transfected with si-h-CPEB4, which corroborated the observed mRNA changes (Fig. 4b). In untransfected, NControl, and si-h-CPEB4 cells, proliferation rate and colony formation and Matrigel invasion assays were markedly inhibited after CPEB4 knockdown ($p<0.01$, Fig. 4c, d, e). Collectively, these data suggest that CPEB4 plays a key role in anchorage-independent growth and the invasiveness of astrocytic tumor cells.

## Vimentin expression is regulated by CPEB4 in astrocytic tumors

To investigate the mechanism of CPEB4 that regulates the malignancy of astrocytotic tumors, we performed co-immunoprecipitation experiment and further analyzed the differential band we observed in the gel. We identified five candidate proteins (Keratin, HSPA5, Mortalin, Vimentin, and Actin) that may be binded by the CPEB4 according to the mass spectrum analysis result (Fig. 5a), and a significant decrease in Vimentin protein expression was observed in the si-h-CPEB4
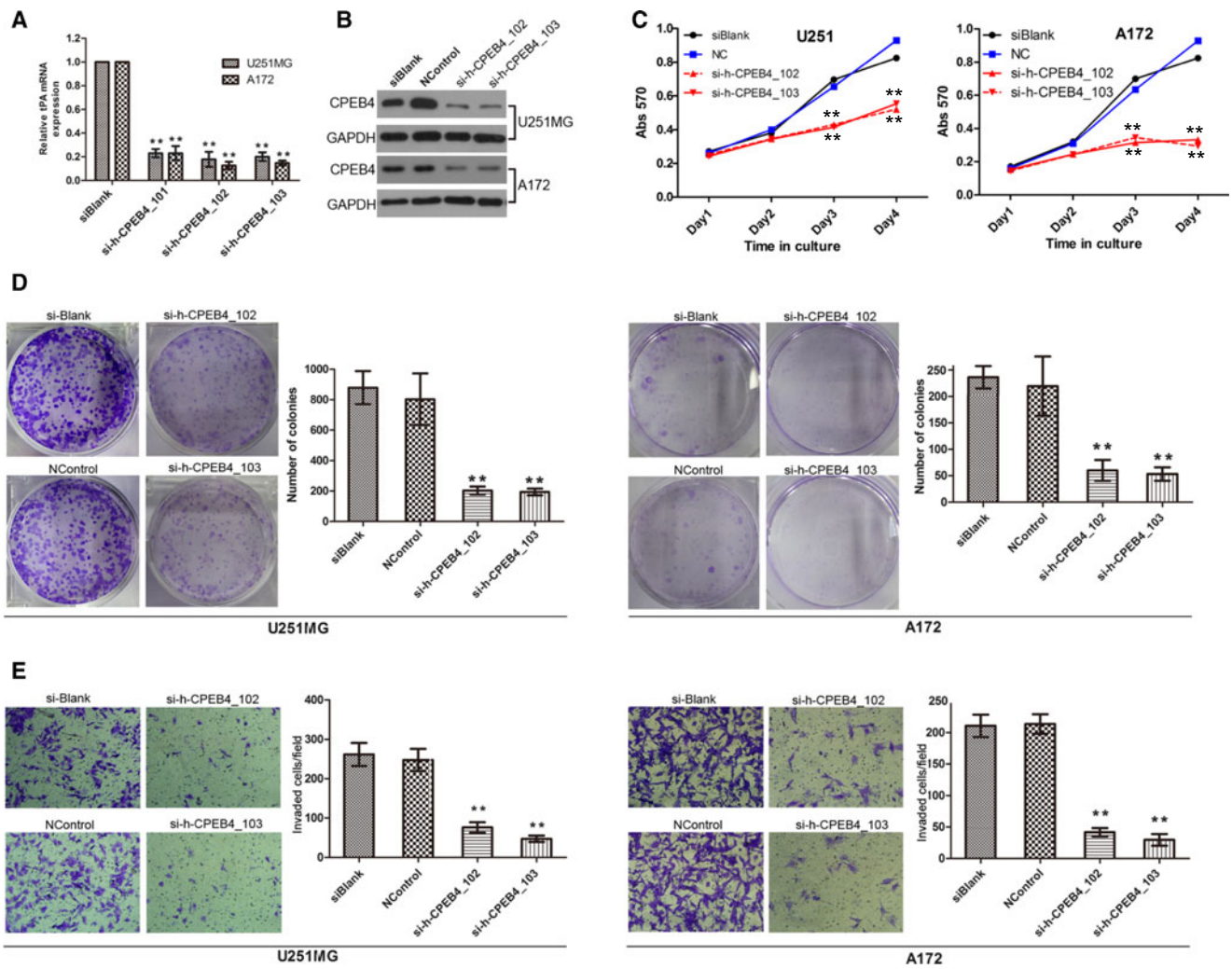
**Fig. 4** Characterization of the effects of CPEB4 knockdown in glioblastoma cells. **a** The expression of CPEB4 mRNA were efficiently downregulated in three different CPEB4-targeting si-h-RNAs (si-h-CPEB 4_101 through si-h-CPEB4_103) and the parental glioblastoma cells transfected with NControl. Data are presented as mean±SEM for three separate experiments performed in duplicate. The *p* values (determined by Student's *t* test) are relative to NControl cells. $^{**}p<0.05$. The greatest reduction of CPEB4 concentrations si-h-CPEB4_102 and si-h-CPEB4_103 were selected for further experiments. **b** Representative experiment of Western blot analysis (*n*=3). Downregulation of CPEB4 protein concentrations in control cells and in cells transfected with si-h-CPEB4 agreed with the mRNA changes. GAPDH concentrations are shown as the loading control. **c** MTT assay analysis shown that the proliferation rate was similar in untransfected, NControl, and si-h-CPEB4 cells. Values are mean±SEM. *Abs 570* absorbance at 570 nm. **d** Representative crystal violet staining of the colonies of U251MG and A172 glioblastoma cells expressing NControl or si-h-CPEB4. The number of colonies (mean±SEM) after 2 weeks of three independent experiments is shown in the right graph, *p* values (determined by Student's *t* test) are relative to NControl cells. $^{**}p<0.05$. **e** The percentages of invaded cells were markedly reduced after CPEB4 knockdown in U251MG and A172 glioblastoma cells. Values (mean± SEM) are the mean numbers of cells per six fields per membrane of three separate experiments and are expressed as percentage of control. $^{**}p<0.05$

cells (Fig. 5b). To investigate whether CPEB4 physically associates with Vimentin, we carried out co-immunoprecipitation with specific anti-CPEB4 and anti-Vimentin antibodies. The interaction of CPEB4 with Vimentin was further demonstrated by reverse endogenous co-immunoprecipitation of Vimentin with CPEB4, supporting a physical CPEB4-Vimentin interaction in vitro (Fig. 6a). To examine the intracellular locations of CPEB4 and Vimentin, expression of both proteins in blank and NC and si-h-CPEB4 cells was visualized by fluorescence microscopy. As shown in

Fig. 6b, in blank and NC groups, CPEB4 was expressed in the cytoplasm, with Vimentin in the same cytoplasmic distribution showing exact co-localization with CPEB4, and the co-localization disappeared when CPEB4 was knocked down. These results indicate that the interaction between CPEB4 and Vimentin takes place in astrocytic tumor cell cytoplasm. We confirmed these results in 12 paired astrocytic tumor samples, and the results showed a positive correlation between protein expression levels of CPEB4 and Vimentin (*p*=0.032, R=0.375, Fig. 7a, b). These data suggest that Vimentin may

**Fig. 5** Purification of CPEB4
protein and mass spectrometry
analysis. **a** Annotated bands
correspond to proteins of interest
selected for MS identification.
Five prominent protein bands
were identified by mass
spectrometry analysis as GRP78
(78 kDa), Mortalin (70 kDa),
Keratin (60 kDa), Vimentin
(54 kDa), and β-actin (42 kDa).
**b**, **c** Western blot analysis on the
interest proteins identified by
mass spectrometry analysis.
Vimentin is significantly reduced
when CPEB4 was knocked down
(*** $p < 0.001$), while the others
had no change
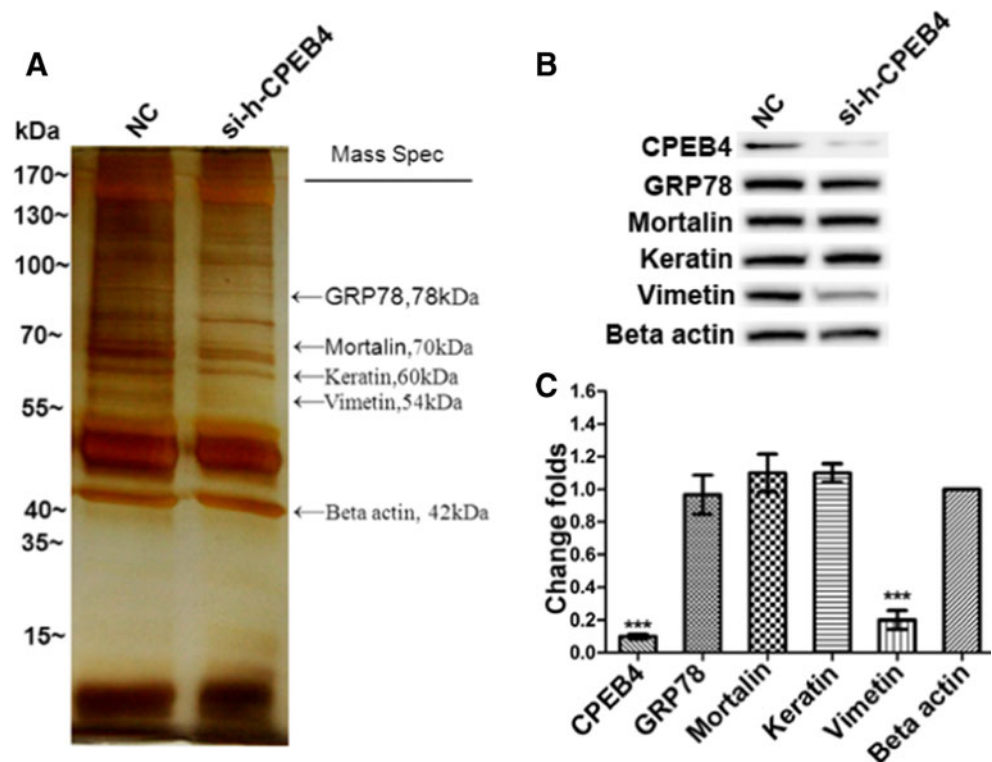


be regulated by CPEB4-mediated translational control in as-
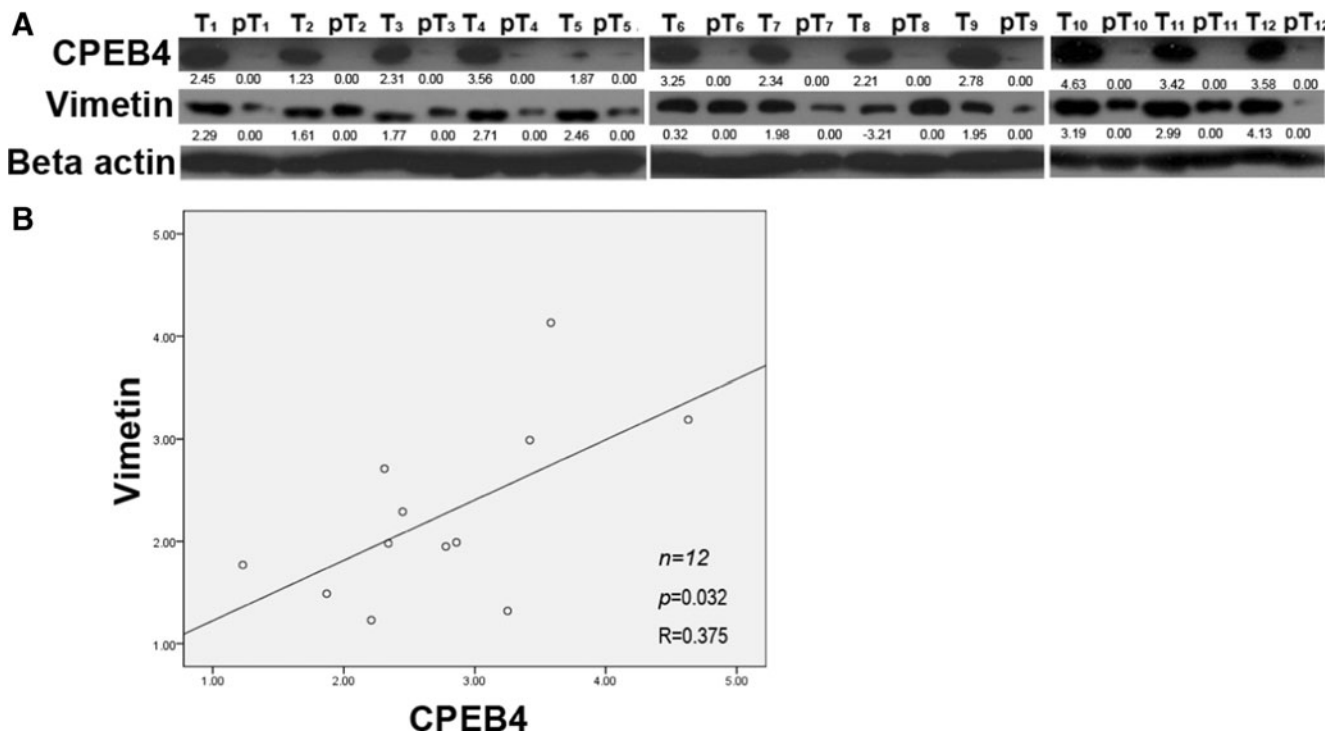trocytic tumor tissues.

## Discussion

The postt ranscriptional regulation of specific mRNA subpop-
ulations has been found to play an important role in changing

the expression of genes responsible for cell tumoral properties
and has been recognized as a critical mechanism in tumori-
genesis in recent years. Recently, new data have demonstrated
that cytoplasmic polyadenylation element binding protein 4
(CPEB4), which can act either as a translational repressor or
activator regulating mitotic and meiotic cell cycles and senes-
cence, has proved to be a key protein in post-transcriptional
gene regulation in the progression of pancreatic carcinoma

**Fig. 6** Protein interactions
between CPEB4 and Vimentin. **a**
Co-immunoprecipitation analysis
shows endogenous CPEB4 co-
immunoprecipitated with
endogenous Vimentin. **b**
Immunofluorescence analysis
showed co-localization between
protein CPEB4 and Vimentin.
Nuclei were counterstained with
DAPI (*blue*). In blank and NC
groups, CPEB4 was expressed in
the cytoplasm and Vimentin in the
same cytoplasmic distribution
showing exact co-localization
between Vimentin with CPEB4,
and the co-localization
disappeared when CPEB4 was
knocked down
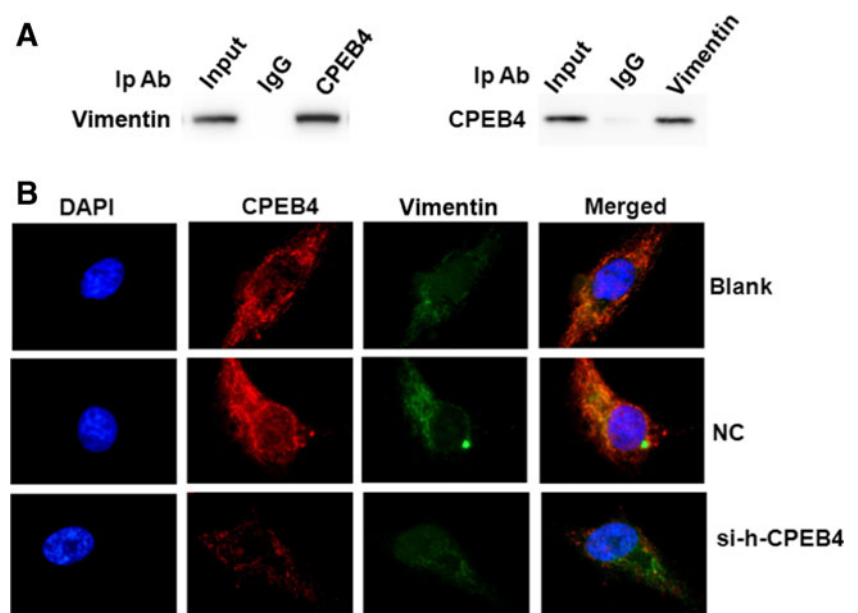
Fig. 7 A positive correlation between protein expression levels of CPEB4 and Vimentin in astrocytic tumor tissues. **a** Western blot analysis on the expression of CPEB4 and Vimentin in 12 paired astrocytic tumor cases. Beta actin was used as normalization control. **b** In 12 paired astrocytic tumor cases, a positive correlation between the protein expression levels of CPEB4 and Vimentin ($p=0.032$, $R=0.375$) was observed. Expression levels were normalized with β-actin

and glioblastoma [19–22]. However, few studies have been performed in astrocytic tumors to examine CPEB4 expression and progression or patient survival.

In this study, we examined the expression of CPEB4 mRNA and protein levels in astrocytic tumors and paired adjacent normal tissues using qRT-PCR and Western blotting, respectively. The mRNA and protein expression of CPEB4 was found to be frequently upregulated in astrocytic tumors when compared to paired normal brain tissues. Next, we performed CPEB4 immunohistochemistry on a large cohort of astrocytic tumor samples (160 cases) with complete clinicopathological and follow-up data. We constructed X-tile plots for the evaluation of scores and divided CPEB4 expression into two populations (a low-expression and high-expression group) in which we corrected for the use of minimum $p$ statistics using the Miller-Siegmund $p$ value correction [23]. ROC analysis for different clinicopathological features and CPEB4 expression was also performed to evaluate survival status. In a univariate study, high CPEB4 expression in astrocytic tumors was associated with a poor survival status ($p<0.001$, Table 2, Fig. 3c). Importantly, we also proved that upregulation of CPEB4 in astrocytic tumors was an independent predictor of shorter overall survival using Kaplan–Meier curves and multivariable Cox proportional hazard regression analysis (relative risk 4.5, 95 % CI 2.1–11.2, $p=0.001$, Table 2). The ROC results confirmed the promising predictive value of CPEB4 with regards to specific survival in all patients with astrocytic tumors (AUC=0.746, $p<0.001$, Fig. 3d). These findings validated the key contributions of CPEB4 in the progression of patients with astrocytic tumors.

In our functional studies on astrocytic tumor cell lines, we found that proliferation (Fig. 4c), colony formation (Fig. 4d), and Matrigel invasion (Fig. 4e) were significantly inhibited after CPEB4 knockdown, suggesting that CPEB4 may promote astrocytic tumor progression by increasing proliferation and anchorage-independent growth and invasiveness.

Furthermore, we detected the interaction between CPEB4 and Vimentin by using co-immunoprecipitation analysis and immunofluorescence staining, and the results have shown that CPEB4-Vimentin takes place in astrocytic tumor cytoplasm (Figs. 5 and 6). When CPEB4 expression was suppressed by si-h-RNA, the expression of the Vimentin protein was negated (Fig. 5b), and the results were also confirmed in the 12 paired astrocytic tumor cases that showed a positive correlation between CPEB4 protein expression levels and Vimentin ($p=0.032$, $R=0.375$) (Fig. 7). These data indicate that Vimentin may be regulated by CPEB4-mediated translational control in astrocytic tumors, which was reported for the first time in astrocytic tumors.

Regarding the function of the CPEB4 gene, as a candidate oncogene, CPEB4-mediated reprogramming of gene expression plays a crucial role in tumorigenesis. The previous studies

showed that CPEB4 expression is upregulated in pancreatic cancer and that heightened CPEB4 expression could facilitate tissue plasminogen activator mRNA expression, promoting the progression of pancreatic tumor proliferation, migration, invasion, and vascularization [24–26]. In pancreatic cancer, CPEB4 also targets many other mRNAs that function in tumorigenesis, including BCL2, SMAD3, and matrix metallopeptidase 7 (MMP7), indicating that CPEB4 might impact tumor progression in several ways [16, 17, 27, 28]. Furthermore, overexpression of CPEB4 and its contribution to tumor progression were detected not only in pancreatic cancer but also found in glioblastoma, suggesting that CPEB4 mediated reprogramming of gene expression during post-translational regulation might be a general mechanism in tumor development [13, 14, 19, 21, 22, 29, 30]. However, our current study revealed that Vimentin is regulated by CPEB4 in astrocytic tumors. As a major constituent of the intermediate filament family of proteins, Vimentin is overexpressed in various epithelial cancers, including prostate cancer, gastrointestinal tumors, tumors of the central nervous system, breast cancer, malignant melanoma, and lung cancer. Vimentin's overexpression in cancer correlates well with accelerated tumor growth, invasion, and poor prognosis.

In conclusion, this work suggests that CPEB4 is an independent prognostic factor and could be used to identify astrocytic tumor patients at high risk of a poor clinical outcome. Furthermore, the potential for developing CPEB4 as a candidate therapeutic target for astrocytic tumors should be further investigated. The discovery of the interaction between CPEB4 and Vimentin might provide us a new insight for gene targeted tumor-specific therapy in astrocytic tumors.

**Conflicts of interest** None

## References

1. Gandini NA, Fermento ME, Salomon DG, Obiol DJ, Andres NC, Zenklusen JC, et al. Heme oxygenase-1 expression in human gliomas and its correlation with poor prognosis in patients with astrocytoma. Tumor Biol. 2014;35(3):2803–15.
2. Dolecek TA, Propp JM, Stroup NE, Kruchko C. CBTRUS statistical report: primary brain and central nervous system tumors diagnosed in the United States in 2005–2009. Neuro Oncol. 2012;14 Suppl 5:v1–49.
3. Smoll NR, Schaller K, Gautschi OP. Long-term survival of patients with glioblastoma multiforme (GBM). J Clin Neurosci. 2013;20(5): 670–5.
4. Towia A, Libermann HRN, Nissim R, Richard K, Irit L, Hermona S, et al. Amplification, enhanced expression and possible rearrangement of EGF receptor gene in primary human brain tumours of glial origin. Nature. 1985;313:144–7.
5. Yin SMEV, Gliomas Á, Apoptosis ÁSÁ, Cell Á. p53 Pathway alteration in brain tumors. Humana Press. 2009.
6. Koul D, Shen R, Shishodia S, Takada Y, Bhat KP, Reddy SA. PTEN down regulates AP-1 and targets c-fos in human glioma cells via PI3-kinase/Akt pathway. Mol Cell Biochem. 2007;300(1–2): 77–87.
7. Zhao S, Lin Y, Xu W, Jiang W, Zha Z, Wang P, et al. Glioma-derived mutations in IDH1 dominantly inhibit IDH1 catalytic activity and induce HIF-1alpha. Science. 2009;324(5924):261–5.
8. Yang M, Yuan Y, Zhang H, Yan M, Wang S, Feng F, et al. Prognostic significance of CD147 in patients with glioblastoma. J Neurooncol. 2013;115(1):19–26.
9. Lin W, Li XM, Zhang J, Huang Y, Wang J, Jiang XF, et al. Increased expression of the 58-kD microspherule protein (MSP58) is correlated with poor prognosis in glioma patients. Med Oncol. 2013;30(4):677.
10. Nuno M, Birch K, Mukherjee D, Sarmiento JM, Black KL, Patil CG. Survival and prognostic factors of anaplastic gliomas. Neurosurgery. 2013;73(3):458–65.
11. Shibahara I, Sonoda Y, Saito R, Kanamori M, Yamashita Y, Kumabe T, et al. The expression status of CD133 is associated with the pattern and timing of primary glioblastoma recurrence. Neuro Oncol. 2013;15(9):1151–9.
12. Mendez R, Richter JD. Translational control by CPEB: a means to the end. Nat Rev Mol Cell Biol. 2001;2(7):521–9.
13. Richter JD. CPEB: a life in translation. Trends Biochem Sci. 2007;32(6):279–85.
14. Burns DM, Richter JD. CPEB regulation of human cellular senescence, energy metabolism, and p53 mRNA translation. Genes Dev 2008;2 2(24): 3449–3460.
15. Eliscovich C, Peset I, Vernos I, Mendez R. Spindle-localized CPE-mediated translation controls meiotic chromosome segregation. Nat Cell Biol. 2008;10(7):858–65.
16. Livingstone M, Atas E, Meller A, Sonenberg N. Mechanisms governing the control of mRNA translation. Phys Biol. 2010;7(2): 021001.
17. Pique M, Lopez JM, Foissac S, Guigo R, Mendez R. A combinatorial code for CPE-mediated translational control. Cell. 2008;132(3):434–48.
18. Kononen J, Bubendorf L, Kallioniemi A, Barlund M, Schraml P, Leighton S, et al. Tissue microarrays for high-throughput molecular profiling of tumor specimens. Nat Med. 1998;4(7):844–7.
19. Kan MC, Oruganty-Das A, Cooper-Morgan A, Jin G, Swanger SA, Bassell GJ, et al. CPEB4 is a cell survival protein retained in the nucleus upon ischemia or endoplasmic reticulum calcium depletion. Mol Cell Biol. 2010;30(24):5658–71.
20. Novoa I, Gallego J, Ferreira PG, Mendez R. Mitotic cell-cycle progression is regulated by CPEB1 and CPEB4-dependent translational control. Nat Cell Biol. 2010;12(5):447–56.
21. Ortiz-Zapater E, Pineda D, Martinez-Bosch N, Fernandez-Miranda G, Iglesias M, Alameda F, et al. Key contribution of CPEB4-mediated translational control to cancer progression. Nat Med. 2012;18(1):83–90.
22. Xu H, Liu B. CPEB4 is a candidate biomarker for defining metastatic cancers and directing personalized therapies. Med Hypotheses. 2013;81(5):875–7.
23. Robert L. Camp MD-FaDLR. X-Tile: a new bio-informatics tool for biomarker assessment and outcome-based cut-point optimization. Clin Cancer Re 10: 7252–7259.
24. Paciucci R, Tora M, Diaz VM, Real FX. The plasminogen activator system in pancreas cancer: role of t-PA in the invasive potential in vitro. Oncogene. 1998;16(5):625–33.

25. Blasi F, Sidenius N. The urokinase receptor: focused cell surface proteolysis, cell adhesion and signaling. FEBS Lett. 2010;584(9): 1923–30.

26. Saaf AM, Halbleib JM, Chen X, Yuen ST, Leung SY, Nelson WJ, et al. Parallels between global transcriptional programs of polarizing Caco-2 intestinal epithelial cells in vitro and gene expression programs in normal colon and colon cancer. Mol Biol Cell. 2007;18(11):4245–60.

27. Sonenberg N, Hinnebusch AG. Regulation of translation initiation in eukaryotes: mechanisms and biological targets. Cell. 2009;136(4):731–45.

28. Gandin V, Miluzio A, Barbieri AM, Beugnet A, Kiyokawa H, Marchisio PC, et al. Eukaryotic initiation factor 6 is rate-limiting in translation, growth and transformation. Nature. 2008;455(7213): 684–8.

29. Tsai LY, Chang YW, Lin PY, Chou HJ, Liu TJ, Lee PT, et al. CPEB4 knockout mice exhibit normal hippocampus-related synaptic plasticity and memory. PLoS one. 2013;8(12):e84978.

30. Theis M, Si K, Kandel ER. Two previously undescribed members of the mouse CPEB family of genes and their inducible expression in the principal cell layers of the hippocampus. Proc Natl Acad Sci U S A. 2003;100(16):9602–7.